# Late Gadolinium Enhancement Imaging in Assessment of Myocardial Viability

## Techniques and Clinical Applications

Laura Jimenez Juan, MD[a,b], Andrew M. Crean, MD[a,c,d,e], Bernd J. Wintersperger, MD[a,c,*]

**KEYWORDS**

• Magnetic resonance imaging • Heart • Myocardial viability • Late gadolinium enhancement • Delayed enhancement • Microvascular obstruction • Thrombus • Revascularization

**KEY POINTS**

- Magnetic resonance imaging allows reliable assessment of the extent of nonviable and viable myocardium after myocardial infarction.
- Late gadolinium enhancement imaging allows transmural differentiation of viable versus nonviable myocardium.
- Late gadolinium enhancement imaging allows prediction of functional recovery after revascularization in obstructive coronary artery disease.
- Besides assessment of myocardial viability, late gadolinium enhancement imaging provides additional insight in potential complications of myocardial infarction.

## INTRODUCTION

Within just over a decade late gadolinium enhancement (LGE) imaging has become a mainstay of cardiac magnetic resonance (MR) imaging supported by extensive study data showing the precision with which the technique identifies nonsalvageable myocardium. It also now plays a key role in differential diagnosis of ischemic and nonischemic cardiomyopathies.[1–3]

Although the exact role of preoperative viability testing remains controversial, many physicians continue to think that clinical decision making in high-risk patients warrants assessment of myocardial viability and the probable myocardial response to revascularization.[4]

However, LGE imaging remains in competition with other established imaging modalities. This article focuses on technical aspects of LGE imaging as well as on the clinical use and impact of the technique in the light of the current multimodality cardiac imaging environment.

## TECHNIQUES AND IMPLEMENTATION

Although postcontrast imaging methods for imaging of myocardial infarction using contrast-enhanced MR imaging date back to the early

[a] Department of Medical Imaging, University of Toronto, Toronto, Ontario, Canada; [b] Department of Medical Imaging, Sunnybrook Health Science Centre, Toronto, Ontario, Canada; [c] Department of Medical Imaging, Peter Munk Cardiac Center, Toronto General Hospital, 585 University Avenue, Toronto, Ontario M5G 2N2, Canada; [d] Department of Medicine, University of Toronto, Toronto, Ontario, Canada; [e] Division of Cardiology, Peter Munk Cardiac Center, Toronto General Hospital, Toronto, Ontario, Canada

* Corresponding author. Department of Medical Imaging, Toronto General Hospital, 585 University Avenue, Toronto, Ontario M5G 2N2, Canada.

*E-mail address:* bernd.wintersperger@uhn.ca

Radiol Clin N Am 53 (2015) 397–411

http://dx.doi.org/10.1016/j.rcl.2014.11.004

0033-8389/15/$ – see front matter 

1980s the underlying theoretic basis of differential enhancement patterns had already been studied in the late 1970s using computed tomography (CT) imaging.[5,6] Development of fast MR imaging techniques and groundbreaking investigations in the late 1990s and early 2000s pushed the boundaries of postcontrast imaging of myocardial infarction.[7,8]

## Contrast Mechanism and Imaging Sequence Techniques

### Underlying principles of contrast agent dynamics

Basic knowledge of the pharmacokinetics of extracellular gadolinium-based contrast agents (GBCAs) is important for a better understanding of LGE imaging techniques. After GBCA bolus injection, extravasation into the interstitial (extracellular-extravascular) space (including myocardium) occurs along a gradient (wash-in) and only reverses (wash-out) over time with continuous renal excretion of GBCA. These processes have been found to be altered in the setting of myocardial infarction.[9–11] Together with a markedly increased GBCA distribution volume based on cell membrane ruptures in acute myocardial infarction (AMI) and the large extracellular space of collagen matrices in chronic myocardial infarction (CMI), these changes result in GBCA accumulation in the infarct area.[12–16] Differences in GBCA concentrations between normal (viable) and infarcted (nonviable) myocardium result in proportional alterations of the relaxivity rate R1 (1/T1).[17,18]

### Principles of imaging sequence techniques

**Optimizing image contrast** T1-weighted imaging techniques are used for assessment of R1 differences in infarct and viability assessment. After initial use of spin-echo techniques, the application of gradient echo sequences speeded up imaging and resulted in improved image quality of the contrast-enhanced imaging of myocardial infarction. The push toward the modern practice of LGE imaging dates back to the implementation of strong T1-weighted inversion recovery (IR) gradient recalled echo (GRE) techniques in the early 2000s.[19] With appropriate inversion time (TI) selection, such techniques enable a ~5-fold difference in signal intensity between viable and nonviable myocardium (**Fig. 1**). Although TI settings may be affected by various factors (**Table 1**) and were initially based on empirical knowledge and user expertise, T1 scouts improve accuracy and ensure adequate nulling of viable or remote myocardium, whereas infarcted/nonviable myocardium is typically displayed with prominent hyperenhancement (**Fig. 2**).[20] Kellman and colleagues[21,22] implemented additional phase-sensitive image reconstruction techniques (PSIR) that have been shown to also permit quantification of infarct sizes with less dependency on optimized TI settings (**Fig. 3**).[21–23]

**Data acquisition strategies** Cardiac MR imaging now enables a variety of different acquisition strategies for LGE imaging that allow tailoring to the individual situation and patient. In most situations coverage of the ventricular myocardium in short-axis orientation with additional single-slice long-axis views in 4-chamber, 2-chamber, and 3-chamber orientation is sufficient. This coverage is commonly achieved with two-dimensional (2D) techniques using noncontiguous coverage and LGE slices matching cine steady-state free precession (SSFP) slice locations (**Table 2**).

Segmented data sampling strategies, which acquire a few k-space lines/heartbeat, are most commonly used but result in multiheartbeat breath-hold periods per single 2D LGE slice.[19] In combination with phase-sensitive IR, such strategies result in a prolonged acquisition time for ventricular coverage and multiorientation acquisition. In patients with breath-hold limitations or cardiac arrhythmia, those techniques are likely to fail.

As an alternative, single slices may be acquired within a single heartbeat using single-shot techniques. Those techniques can also be applied during shallow breathing and allow ventricular coverage in ~2 breath holds but at the cost of lower spatial and temporal resolution (**Fig. 4**, see **Table 2**). In order to maintain adequate signal/noise ratio (SNR) and contrast/noise ratio (CNR), these approaches typically use an SSFP data read-out.[24,25] In general, single-shot techniques showed excellent correlation of infarct extent compared with segmented techniques.[24–26] Respiratory gating using Navigator techniques may be used as alternatives in the setting of stable sinus rhythm.[27]

Despite the high image quality of 2D techniques, various three-dimensional (3D) techniques have become available covering the ventricles in a single volume either using respiratory-gated or breath-held approaches.[28,29] Three-dimensional IR GRE approaches showed superior SNR, CNR, and image quality with improved delineation of nontransmural hyperenhancement and subtle involvement of papillary muscles.[30,31] However, using 3D respiratory-gated LGE imaging, proper myocardial nulling remains challenging because data sampling continues for minutes and TI settings may not remain optimal throughout acquisition (**Fig. 5**, see **Table 2**).

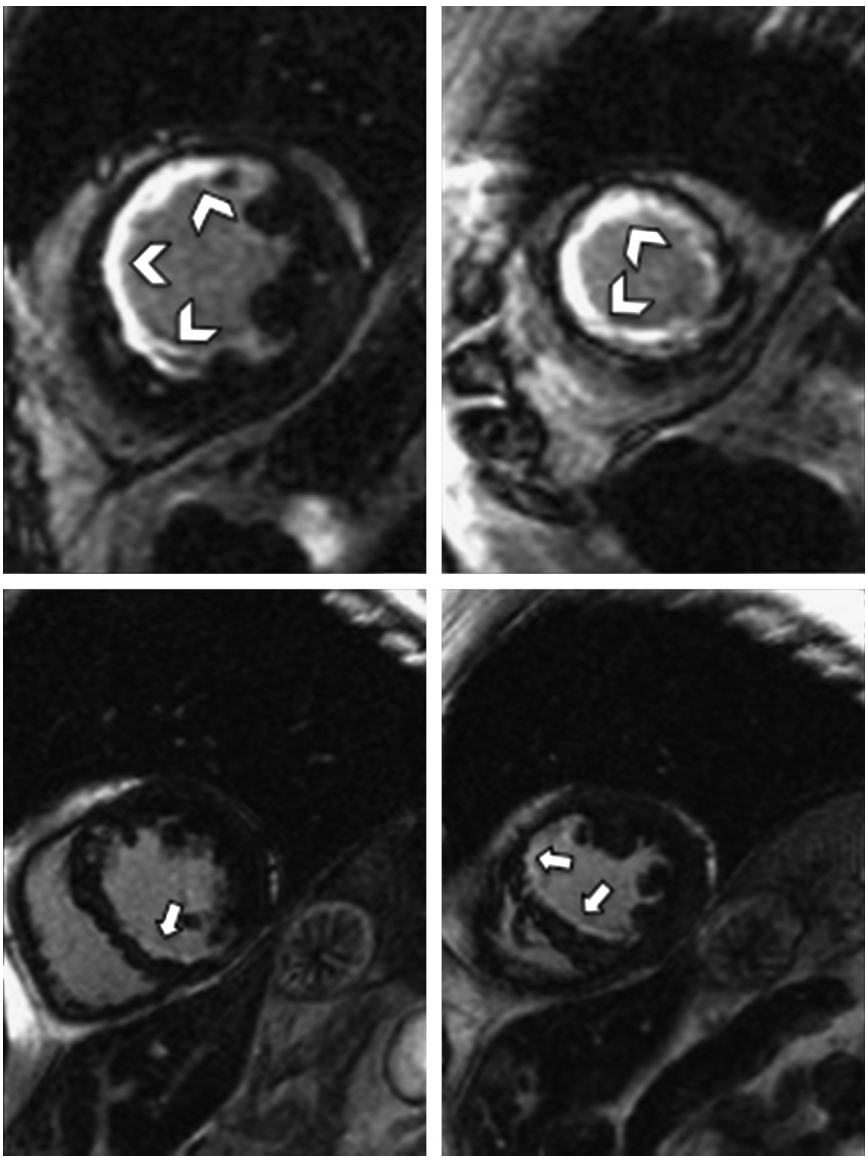

Fig. 1. Short-axis LGE data sets of 2 cases with (*upper row*) extensive near transmural myocardial infarction (*arrowheads*) and (*lower row*) subtle subendocardial infarction (*arrows*).

### *Contrast agents, dosing, and imaging timing*

GBCA selection and contrast dosing may affect exact imaging parameters and timing in LGE imaging because various factors affect tissue T1 properties (see **Table 1**; **Table 3**).

In recent years, various extracellular GBCAs have become generally available for use in MR imaging. With respect to the use of a specific GBCA for cardiac MR, and especially LGE imaging, users need to refer to their respective authorities.

Extracellular GBCA can generally be classified using various criteria. The following have been identified as criteria potentially influencing LGE imaging:

- GBCA concentration
- Protein-binding capabilities

Together with other characteristics, these factors may result in differences of GBCA R1 and R2 properties, potentially affecting signal characteristics in LGE imaging.

Various comparative studies have shown differences between agents as a result of different R1,

**Table 1**
**Influencing factors of postcontrast myocardial T1 and TI in LGE imaging**

| | |
|---|---|
| GBCA R1 relaxivity | Higher GBCA R1 relaxivity = ↓ TI[a] |
| GBCA volume | Higher GBCA volume = ↓ TI[b] |
| Time after GBCA application | Shorter wait time = ↓ TI[c] |
| Magnetic field strength ($B_0$) | Higher $B_0$ = ↑ TI |

[a] Assumes otherwise identical GBCA.
[b] Assumes volume differences of the identical GBCA (with stable remaining factors).
[c] Also higher rate of T1 change early after injection potentially requiring repeated TI adjustment.

doses, or protein-binding capabilities but generally enable reliable identification and delineation of infarcted, nonviable tissue (see **Table 3**).[32–38]

LGE imaging is typically performed 8 to 20 minutes after contrast application with imaging at higher end dosages (0.15–0.2 mmol/kg body weight) potentially requiring TI adjustments over time to account for contrast agent concentration changes (see **Table 3**). The application of identical imaging techniques in the early stages postinjection (1–5 minutes) is referred to as early gadolinium enhancement (EGE) and may be used for the delineation of specific features in AMI without myocardial nulling (discussed later).

## CLINICAL IMPACT AND OUTCOMES OF LATE GADOLINIUM ENHANCEMENT IMAGING

### *Clinical Importance of the Assessment of Myocardial Viability*

Risk stratification of patients after AMI is crucial for effective treatment planning. The steady improvement of the outcome of patients with acute coronary syndrome has resulted in a higher incidence of patients with chronic left ventricular (LV) dysfunction. Therefore, there is increasing interest in identifying accurate predictors of outcome that may improve risk stratification and guide management.[39–41]

The differentiation of dysfunctional myocardium as viable or nonviable is an important predictor of outcome after myocardial infarction (**Table 4**).

A multitude of studies have supported the notion that patients with ischemic cardiomyopathy with dysfunctional but still viable myocardium derive prognostic benefit from revascularization and that, conversely, they do poorly if treated medically.[42] In contrast, there is a low likelihood that patients with nonviable myocardium benefit from coronary revascularization.[43,44]

The recent STICH (Surgical Treatment for Ischemic Heart Failure) trial controversially failed to show such an advantage of revascularization compared with optimum medical therapy in patients with ischemic cardiomyopathy.[45] Although the study has been subject to major criticism, including the lack of any viability testing in greater than 50% of patients, subsequent substudies only showed minimal benefit of revascularization in the

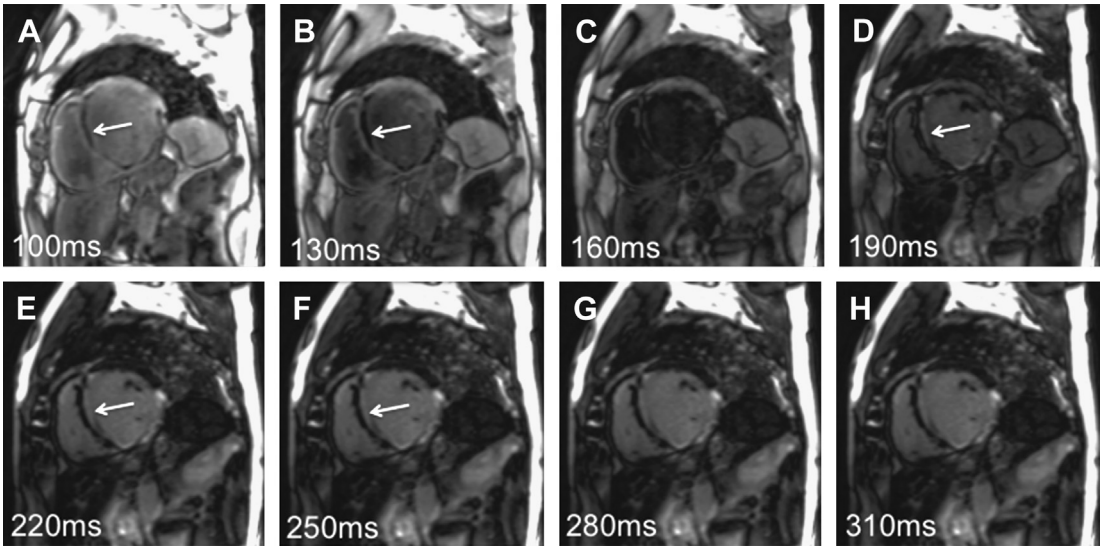


**Fig. 2.** TI scout series (*A–H*) ranging from 100 to 310 milliseconds TI. Note that the zero pass of blood pool (*C*) happens before normal myocardium and that at short TI times (100–160 milliseconds) nonviable infarcted myocardium (*arrows*) is predominately dark and shows optimal nulling at 250 milliseconds (*F*).

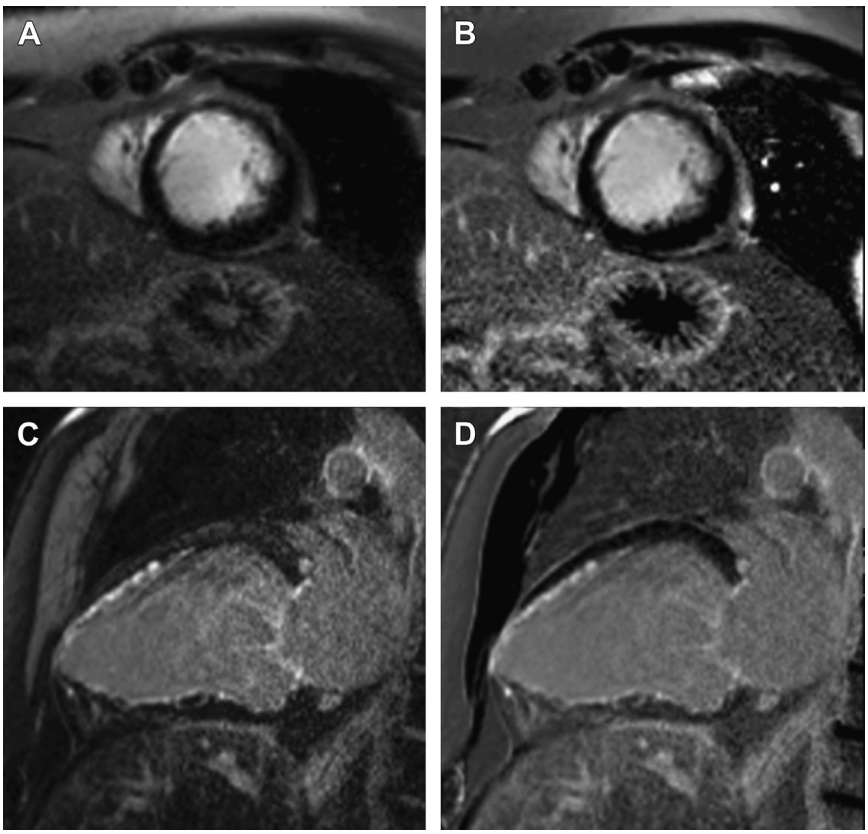


**Fig. 3.** Comparison of magnitude (*A*, *C*) and phase (*B*, *D*) reconstructions in PSIR GRE. Although optimal TI settings show optimized nulling (TI, 280 milliseconds; 3T) in the magnitude display (*A*) with no difference to phase display (*B*) on the short-axis slices, the long-axis example shows dark myocardium in phase reconstruction (*D*) despite nonoptimal (too short) TI (200 milliseconds; 1.5 T) in the magnitude display (*C*).

**Table 2**
**LGE acquisition techniques: benefits and limitations**

| Technique | Benefits | Limitations |
|---|---|---|
| 2D segmented IR GRE | High spatial resolution | Single slice/breath hold<br>Breathing/motion artifacts<br>Arrhythmia artifacts<br>Possibly TI readjustment |
| 2D segmented IR SSFP | High spatial resolution<br>High SNR | Single slice/breath hold<br>Breathing/motion artifacts<br>Arrhythmia artifacts<br>Possibly TI readjustment |
| 2D single-shot IR SSFP | Multiple slices/breath hold or free breathing<br>No arrhythmia artifacts<br>No TI readjustment | Limited spatial resolution<br>Possible image blurring |
| 3D breath-hold IR GRE | Smaller voxel size<br>Fast ventricular coverage<br>Contiguous coverage | Breathing/motion artifacts<br>Arrhythmia artifacts |
| 3D respiratory-gated IR GRE | High spatial resolution<br>Free breathing<br>Higher CNR | Arrhythmia artifacts<br>Nonoptimized nulling |

*Abbreviations:* CNR, contrast/noise ratio; SNR, signal/noise ratio.

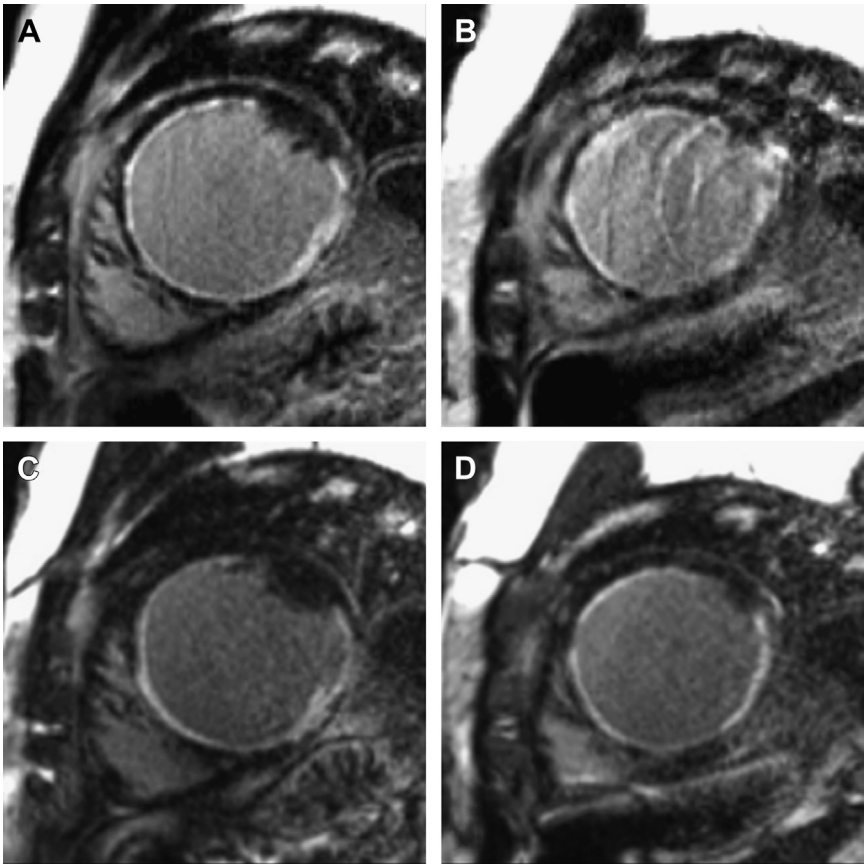


**Fig. 4.** Two-dimensional short-axis segmented IR GRE slices (*A*, *B*) and corresponding 2D single-shot SSFP slices (*C*, *D*) in the same patient. Although segmented IR GRE shows artifacts (*B*), the corresponding single-shot data are artifact free (*D*).

setting of significant viability.[46] The prospective PARR-2 (PET and Recovery Following Revascularization) trial, with the inclusion of viability assessment by means of PET, also failed to show a difference in primary outcome, whereas the local Ottawa-FIVE (18F-FDG PET Imaging of Myocardial Viability in an Experienced Center with Access to 18F-FDG and Integration with Clinical Management Teams) PARR-2 substudy confirmed a significant outcome benefit in the PET-guided group.[47]

## *Prognostic Value of Late Gadolinium Enhancement Imaging After Myocardial Infarction*

Cardiac MR imaging has become a valuable noninvasive tool for the assessment and risk stratification of patients after myocardial infarction. In particular, the contribution of LGE imaging to viability imaging has produced a paradigm shift in the assessment of myocardial viability.[48]

Besides being an important diagnostic tool, LGE imaging is also able to provide prognostic information.[49] There is substantial evidence that the infarct extent assessed by LGE imaging correlates with the likelihood of functional recovery of dysfunctional myocardium after coronary revascularization.[8,50,51]

Furthermore, LGE imaging provides additional parameters related to AMI that may affect patient outcome, such as microvascular obstruction (MVO),[52] thrombus formation[53] and peri-infarct zone.[54] In addition, LGE imaging can easily be combined with stress MR perfusion imaging, allowing the combined evaluation of myocardial viability and ischemia.

Various studies have also shown the high sensitivity of LGE imaging in the identification of otherwise potentially unrecognized non–Q-wave myocardial infarctions.[55–57]

### *Infarct extent and viability*

Using animal experiments with histopathologic validation, Kim and colleagues[7] validated the ability of LGE imaging to distinguish between

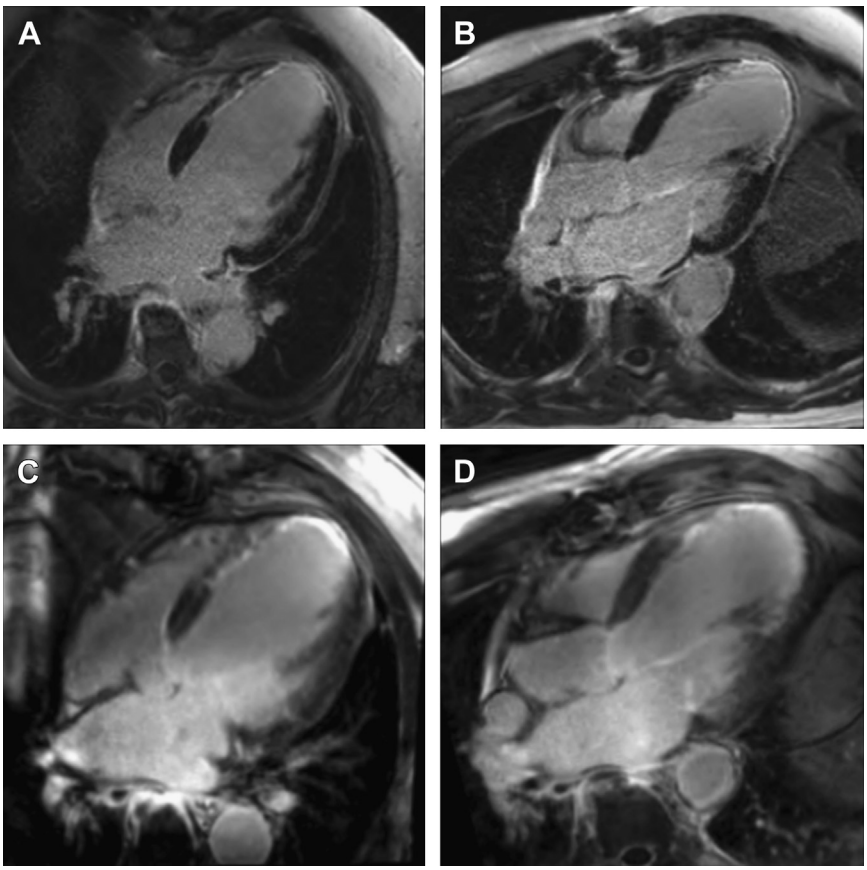


**Fig. 5.** Comparison of 2D LGE (*A*, *B*) and respiratory-gated 3D LGE (*C*, *D*) in a patient with extensive left anterior descending (LAD) infarction. Note the nonnulled viable myocardium in the 3D approach.

ischemic but viable myocardium, which showed no hyperenhancement, versus infarcted myocardium that showed hyperenhancement in AMI and CMI. A human pioneer study showed an inversely proportional relationship between the likelihood of improvement in regional contractility after revascularization and the transmural extent of hyperenhancement in LGE imaging before revascularization.[8]

Since then, multiple cardiac MR studies have been performed with the primary outcome of evaluating the recovery in contractility and LV systolic function after revascularization, based on the amount of viable myocardium.[58–60]

It has been shown that changes in LV ejection fraction after revascularization are linearly correlated with the number of viable segments and baseline amount of scar, resulting in a general

**Table 3**
**Contrast agent selection, dosing, and imaging timing for LGE**

| | | Remarks |
|---|---|---|
| Contrast agent | Extracellular GBCA | Agent with minor protein-binding applicable |
| Contrast volume/dose | 0.1–0.2 mmol/kg BW | Lower dose with high R1 or 1M agents |
| Data acquisition | 8–20 min postinjection[a] | ≥10 min recommended for protein-binding agents[a]; less TI variation over time with later start |

*Abbreviation:* BW, body weight.

[a] With the same contrast injection early gadolinium enhancement imaging may additionally performed 1 to 5 minutes postinjection (eg, thrombus assessment, microvascular obstruction assessment).

**Table 4**
**Myocardial viability: definition of terms**

| | |
|---|---|
| **Viable** | |
| Hibernating myocardium | State of reversible contractile myocardial dysfunction with reduced myocardial perfusion |
| Stunned myocardium | State of reversible contractile myocardial dysfunction with restored myocardial perfusion |
| **Nonviable** | |
| Necrotic/scarred myocardium | Irreversible contractile myocardial dysfunction with tissue necrosis/ replacement scar |

consensus about patient-based criteria for prediction of global LV improvement after revascularization.[60–62] Although no LGE or less than 25% transmurality is the best predictor of recovery, segments with less than 50% of transmural LGE extent are generally considered viable.[63] The latter threshold has also been implemented in current guidelines as an established predictor of significant LV function improvement after coronary revascularization (**Table 5**).[62]

Although it is not routinely part of myocardial viability assessment in cardiac MR,[62,64] several studies have shown the prognostic value of MR stress perfusion in the assessment of myocardial ischemia and an improved accuracy of LGE imaging in viability imaging.[51,65–67]

### *Microvascular obstruction*

MVO or the no-reflow phenomenon is defined as an area of nonviable tissue within the infarct core mainly related to microvascular injury with endothelial swelling/blebs. As a result, there is substantial limitation of blood flow despite successful revascularization of the epicardial vasculature.[68]

MVO only occurs in acute infarcts and it is not typically seen in CMI. It therefore helps to determine the acuity of the myocardial infarction (see **Table 5**). Wu and colleagues[52] found that MVO persists for at least 9 days after the infarction and it resolves completely in 6 months.

LGE imaging, first-pass perfusion imaging, and EGE imaging are highly sensitive techniques in detecting the characteristic hypoenhanced areas of MVO within the infarcted myocardium, providing important information that is also related to the total infarct size (**Fig. 6**). However, the extent of MVO on these various imaging techniques varies because the contrast agent may gradually diffuse into hypoenhancing cores over time.

Although there are limited data on how MVO affects contractile recovery of the infarct zone,[69] the presence of MVO, in addition to myocardial infarction, is a strong predictor of LV remodeling,[70,71] adverse cardiovascular complications, and poor outcome.[72,73]

### *Thrombus*

Myocardial infarction/scar is a major risk factor for mural thrombus formation which is most common in apical infarcts.[74,75] The detection of LV thrombus is important because of the related high risk of systemic embolization.[76] LGE imaging has 88% sensitivity and 99% specificity for detection of thrombus and it is especially useful in detecting small, apical, and layered thrombi that can easily be missed in echocardiography (**Fig. 7**, see **Table 5**).[53]

**Table 5**
**Checklist for LGE imaging of myocardial infarction and viability**

| LGE Parameter | Description | Clinical Outcome |
|---|---|---|
| Infarct extension | Myocardial involvement of LGE: <50% myocardial thickness; ≥50% myocardial thickness | High likelihood of functional recovery if LGE involves <50% transmural myocardial thickness and >10 viable segments[a] |
| MVO | In acute infarcts, hypoenhanced areas within the infarct core | Predictor of adverse LV remodeling and major cardiovascular events |
| Thrombus | Hypoenhanced intracavitary masses, typically adjacent to myocardial scar | High risk of systemic embolization |
| Peri-infarct zone | Peripheral regions adjacent to the infarct core | Predictor of ventricular tachycardia and mortality |

[a] Based on American Heart Association 16-segment model.

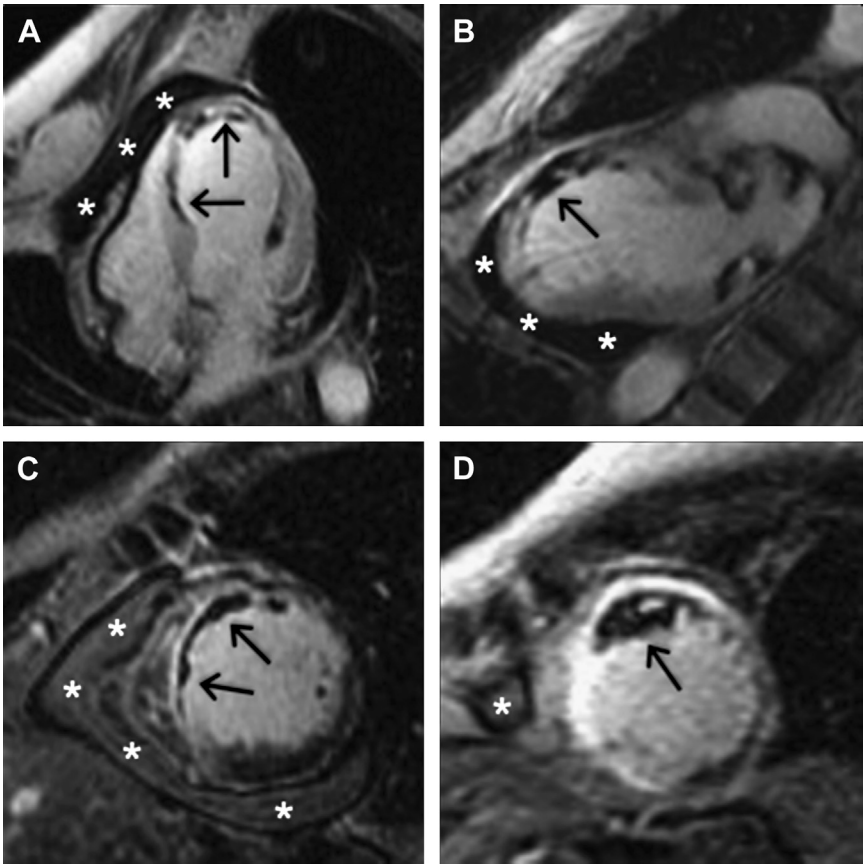


**Fig. 6.** Extensive coronary artery disease imaged before potential coronary revascularization. EGE imaging (*A*, *B*) and LGE imaging (*C*, *D*) show LV dilatation with a laminated thrombus (*arrows*) extending from the midcavity to the anterior apex, adjacent to a transmural LAD infarction. A small pericardial effusion was present (*asterisks*). Previous echocardiography failed to depict the thrombus.

### *Peri-infarct zone*

There is increasing evidence that infarct border characterization may also have important prognostic implications. Although of limited use in clinical practice, LGE imaging has been introduced as a promising tool to differentiate the infarct core and peripheral regions (peri-infarct zone).

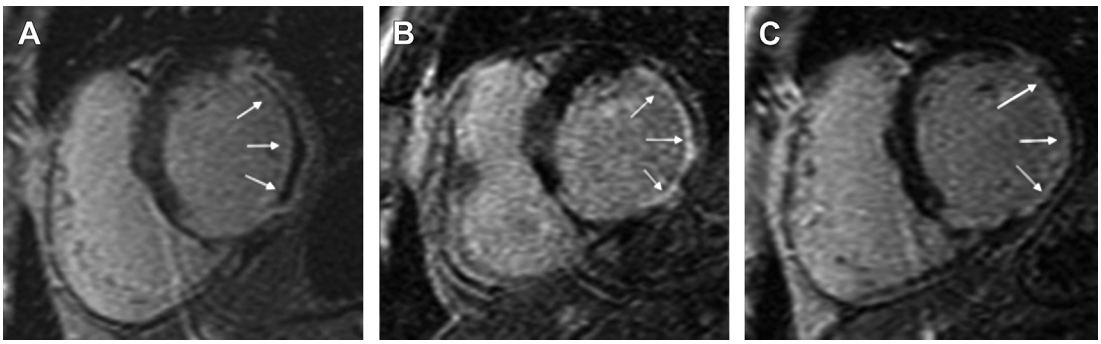


**Fig. 7.** ST-elevation myocardial infarction and ad hoc angioplasty of a totally occluded left circumflex coronary artery. (*A*) LGE imaging within 48 hours showing a large hypoenhanced area within the infarct core compatible with MVO (*arrows*). Follow-up imaging after 1 month (*B*) shows resolution of the MVO, LV wall thinning, and greater than 50% transmural LGE extent consistent with previous myocardial infarction. Further follow-up at 6 months (*C*) shows increased LV wall thinning of the ischemic scar and LV remodeling.

The heterogeneity and extent of the peri-infarct zone morphology is a good predictor of ventricular tachycardia inducibility[77] and has been associated with increased mortality after myocardial infarction,[54] independent of age and LV ejection fraction (see **Table 5**).[78]

## MAGNETIC RESONANCE VIABILITY IMAGING IN THE CONTEXT OF MULTIMODALITY IMAGING: STRENGTHS AND WEAKNESSES

### *Competing and Complementing Modalities in Assessment of Myocardial Viability*

At present, applicable modalities for assessment of myocardial viability may rely on the injection of a tracer/contrast agent or highlight the presence of viability based on functional recovery under pharmacologic challenges. Important aspects to consider when selecting an imaging technique for viability assessment are provided in **Table 6**.

In single-photon emission computed tomography (SPECT), cardiomyocytes retaining radioactive label are, by definition, viable. Thallium (thallium-201) imaging depends on the integrity of the cell membrane Na/K pumps, whereas technetium (Tc-99m) agents relate to mitochondrial integrity. Maximal thallium retention may not occur within the first 3 to 4 hours and therefore may require delayed imaging to assess uptake 24 hours after injection (rest-redistribution). Tc-99m agents relate to mitochondrial integrity and do not redistribute to any great extent but require tracer reinjection for rest distribution imaging. Increased specificity may be achieved by nitrate-enhanced protocols.[79] Because the photon energy of both tracers is low, attenuation artifacts may consequently reduce accuracy. In addition, spatial resolution is limited and thus thinned but hibernating segments may appear as fixed defects. SPECT has also been shown to miss up to ~45% of subendocardial infarctions.[48]

The metabolic signature of viable but oxygen-deplete myocytes, with a switch from fatty acid metabolism to dominance of glucose metabolism, are exploited by PET. Segments with little or no blood flow tracer (eg, N-13 ammonia or Rb-82 Cl) uptake at rest but extensive uptake of [18F]fluorodeoxyglucose PET (18FDG-PET) show a perfusion/metabolism mismatch that is characteristic of hibernating myocardium. Matched defects in blood flow imaging and 18FDG-PET are characteristic of transmural scar/infarct extent. Although PET provides improved spatial resolution, identification of subendocardial infarcts is potentially still limited and again sensitivity is higher than specificity (**Fig. 8**).[80] LGE and 18FDG-PET imaging comparisons have shown general good agreement, with MR imaging showing hyperenhancement in 11% of segments classified as normal by PET.[81]

In echocardiography, residual viability is shown by the presence of a biphasic response to a dobutamine challenge in segments with resting dysfunction. Although hibernating myocardium responds

**Table 6**
**Considerations for viability assessment modality selection**

| | SPECT | FDG-PET | Echocardiography | LGE MR Imaging |
|---|---|---|---|---|
| Underlying mechanism | Perfusion; cellular integrity | Metabolic integrity | Contractile reserve | Perfusion; passive tracer distribution |
| Spatial resolution | + | ++ | ++ | +++ |
| Availability | +++ | + | +++ | ++ |
| Radiation | ++ | ++ | – | – |
| Cost | + | ++ | + | ++ |
| Potential for artifact | ++ | + | ++ | +/– |
| Safe in renal failure | Y | Y | Y | N |
| Safe with pacemaker/AICD | Y | Y | Y | N |
| Influence of body habitus | +++ | ++ | +++ | – |
| Time required | +++ | ++ | + | + |
| Sensitivity | ++ | ++ | ++ | ++ |
| Specificity | + | + | +++ | ++ |
| Supporting data | +++ | ++ | ++ | ++ |

*Abbreviations:* AICD, automatic implantable cardioverter-defibrillator; FDG, [18F]fluorodeoxyglucose; SPECT, single-photon emission computed tomography.

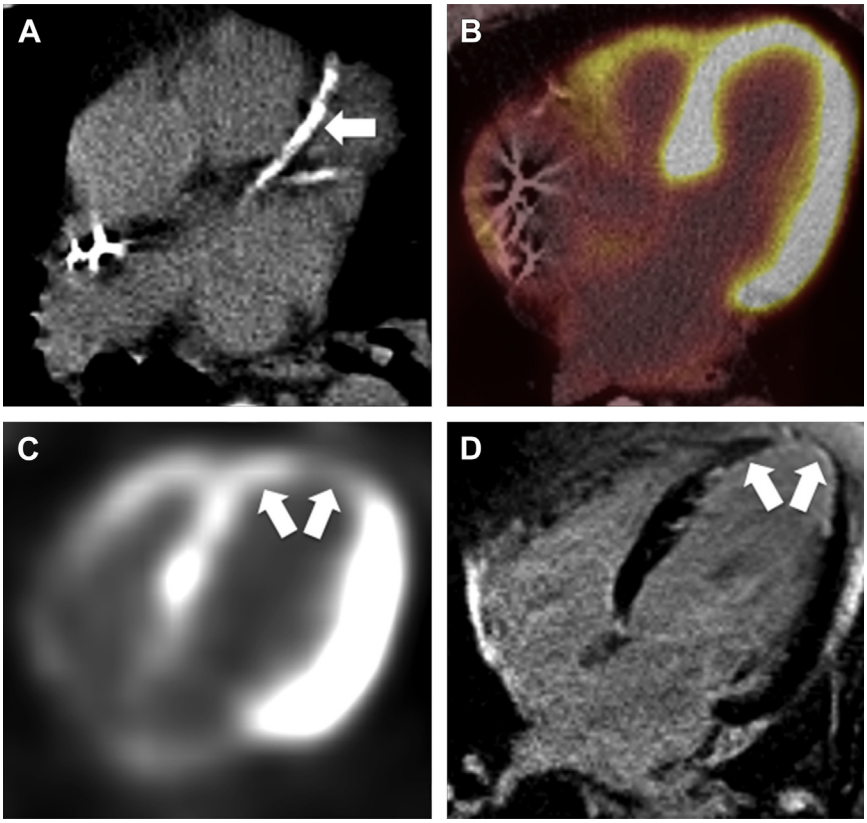


**Fig. 8.** (*A*) Male patient with severe global LV dysfunction and heavily calcified coronary arteries (*arrow*). 18FDG PET study shows normal metabolic activity throughout the left ventricle (*B*), suggesting myocardial viability. (*C*) Female patient with decreased tracer uptake in the distal septum and apex (*arrows*) at 18FDG PET with (*D*) matching hyperenhancing scar on LGE imaging.

with an appearance of improved contractility reserve at low doses of dobutamine (maximum 10 μg/kg/min), segmental function deteriorates again with further dose increase (−40 μg/kg/min). Such a response pattern predicts recovery after revascularization with pooled sensitivity and specificity of 79% and 87% respectively.[82] General echocardiography limitations apply, such as operator dependency and the subjective nature of wall motion interpretation. In addition, echocardiography does not directly visualize the extent of nonviable myocardium.

Low-dose dobutamine cardiac MR was reported to predict functional recovery in a similar way to echocardiography, albeit with improved diagnostic accuracy.[83,84] In addition, simple end-diastolic wall thickness assessment with a threshold of less than 5.5 to 6 mm was used to indicate nonviability in cardiac MR before the LGE era.[85] However, this technique ignores the significant thinning that may occur without scar in hibernating segments.

## New Developments

In recent years, cardiac CT has been explored with regard to viability assessment but for now remains the least-explored technique.[86] As mentioned earlier, basic principles of iodinated contrast agent distribution patterns are similar to LGE MR, leading to the term late iodine enhancement to identify regions of infarcted myocardium.[5,6,87] Limitations to CT viability imaging include radiation dose, the poor CNR compared with LGE MR techniques, and the potential need for a large amount of iodinated contrast agent. The use of dual-energy CT has recently shown promise in animal and patient studies of myocardial infarction.[88–91]

In addition, the development of hybrid MR-PET imaging holds great promise in further improvement of viability assessment and even more precise prediction of functional recovery after revascularization.[92] However, installed bases may limit the use to dedicated research applications. Most importantly, the likely high costs of

such hybrid examinations would demand a clear benefit with respect to the predictive value and specificity of viability assessment.

## SUMMARY

Assessment of myocardial viability is of ever-evolving interest in cardiovascular imaging, with major societies having incorporated viability imaging as class I or class IIa indications in their guidelines to better guide patient management. As with LGE cardiac MR, assessment of residual myocardial viability or the extent of myocardial infarction is straightforward and this technique may easily be combined with other cardiac MR modules. In clinical routine, functional assessment and myocardial perfusion imaging if often used in conjunction allowing for a comprehensive assessment of ischemic heart disease.

## REFERENCES


1. Mahrholdt H, Wagner A, Judd RM, et al. Delayed enhancement cardiovascular magnetic resonance assessment of non-ischaemic cardiomyopathies. Eur Heart J 2005;26(15):1461–74.
2. Cummings KW, Bhalla S, Javidan-Nejad C, et al. A pattern-based approach to assessment of delayed enhancement in nonischemic cardiomyopathy at MR imaging. Radiographics 2009;29(1):89–103.
3. Hunold P, Schlosser T, Vogt FM, et al. Myocardial late enhancement in contrast-enhanced cardiac MRI: distinction between infarction scar and non-infarction-related disease. AJR Am J Roentgenol 2005;184(5):1420–6.
4. Cortigiani L, Bigi R, Sicari R. Is viability still viable after the STICH trial? Eur Heart J Cardiovasc Imaging 2012;13(3):219–26.
5. Siemers PT, Higgins CB, Schmidt W, et al. Detection, quantitation and contrast enhancement of myocardial infarction utilizing computerized axial tomography: comparison with histochemical staining and 99mTc-pyrophosphate imaging. Invest Radiol 1978;13(2):103–9.
6. Higgins CB, Siemers PT, Schmidt W, et al. Evaluation of myocardial ischemic damage of various ages by computerized transmission tomography. Time-dependent effects of contrast material. Circulation 1979;60(2):284–91.
7. Kim RJ, Fieno DS, Parrish TB, et al. Relationship of MRI delayed contrast enhancement to irreversible injury, infarct age, and contractile function. Circulation 1999;100(19):1992–2002.
8. Kim RJ, Wu E, Rafael A, et al. The use of contrast-enhanced magnetic resonance imaging to identify reversible myocardial dysfunction. N Engl J Med 2000;343(20):1445–53.
9. Kim RJ, Chen EL, Lima JA, et al. Myocardial Gd-DTPA kinetics determine MRI contrast enhancement and reflect the extent and severity of myocardial injury after acute reperfused infarction. Circulation 1996;94(12):3318–26.
10. Klein C, Nekolla SG, Balbach T, et al. The influence of myocardial blood flow and volume of distribution on late Gd-DTPA kinetics in ischemic heart failure. J Magn Reson Imaging 2004;20(4):588–93.
11. Klein C, Schmal TR, Nekolla SG, et al. Mechanism of late gadolinium enhancement in patients with acute myocardial infarction. J Cardiovasc Magn Reson 2007;9(4):653–8.
12. Flacke SJ, Fischer SE, Lorenz CH. Measurement of the gadopentetate dimeglumine partition coefficient in human myocardium in vivo: normal distribution and elevation in acute and chronic infarction. Radiology 2001;218(3):703–10.
13. Wendland MF, Saeed M, Arheden H, et al. Toward necrotic cell fraction measurement by contrast-enhanced MRI of reperfused ischemically injured myocardium. Acad Radiol 1998;5(Suppl 1):S42–4 [discussion: S45–6].
14. Arheden H, Saeed M, Higgins CB, et al. Measurement of the distribution volume of gadopentetate dimeglumine at echo-planar MR imaging to quantify myocardial infarction: comparison with 99mTc-DTPA autoradiography in rats. Radiology 1999; 211(3):698–708.
15. Mahrholdt H, Wagner A, Judd RM, et al. Assessment of myocardial viability by cardiovascular magnetic resonance imaging. Eur Heart J 2002;23(8):602–19.
16. Mewton N, Liu CY, Croisille P, et al. Assessment of myocardial fibrosis with cardiovascular magnetic resonance. J Am Coll Cardiol 2011;57(8):891–903.
17. Burstein D, Taratuta E, Manning WJ. Factors in myocardial "perfusion" imaging with ultrafast MRI and Gd-DTPA administration. Magn Reson Med 1991;20(2):299–305.
18. Tweedle MF, Wedeking P, Telser J, et al. Dependence of MR signal intensity on Gd tissue concentration over a broad dose range. Magn Reson Med 1991;22(2):191–4 [discussion: 195–6].
19. Simonetti OP, Kim RJ, Fieno DS, et al. An improved MR imaging technique for the visualization of myocardial infarction. Radiology 2001; 218(1):215–23.
20. Gupta A, Lee VS, Chung YC, et al. Myocardial infarction: optimization of inversion times at delayed contrast-enhanced MR imaging. Radiology 2004; 233(3):921–6.
21. Kellman P, Arai AE, McVeigh ER, et al. Phase-sensitive inversion recovery for detecting myocardial infarction using gadolinium-delayed hyperenhancement. Magn Reson Med 2002;47(2):372–83.
22. Kellman P, Larson AC, Hsu LY, et al. Motion-corrected free-breathing delayed enhancement

imaging of myocardial infarction. Magn Reson Med 2005;53(1):194–200.
23. Huber AM, Schoenberg SO, Hayes C, et al. Phase-sensitive inversion-recovery MR imaging in the detection of myocardial infarction. Radiology 2005; 237(3):854–60.
24. Huber A, Bauner K, Wintersperger BJ, et al. Phase-sensitive inversion recovery (PSIR) single-shot True-FISP for assessment of myocardial infarction at 3 tesla. Invest Radiol 2006;41(2):148–53.
25. Huber A, Hayes C, Spannagl B, et al. Phase-sensitive inversion recovery single-shot balanced steady-state free precession for detection of myocardial infarction during a single breathhold. Acad Radiol 2007;14(12):1500–8.
26. Bauner KU, Muehling O, Wintersperger BJ, et al. Inversion recovery single-shot TurboFLASH for assessment of myocardial infarction at 3 Tesla. Invest Radiol 2007;42(6):361–71.
27. Matsumoto H, Matsuda T, Miyamoto K, et al. Feasibility of free-breathing late gadolinium-enhanced cardiovascular MRI for assessment of myocardial infarction: navigator-gated versus single-shot imaging. Int J Cardiol 2013;168(1):94–9.
28. Nguyen TD, Spincemaille P, Weinsaft JW, et al. A fast navigator-gated 3D sequence for delayed enhancement MRI of the myocardium: comparison with breathhold 2D imaging. J Magn Reson Imaging 2008;27(4):802–8.
29. Bauner KU, Muehling O, Theisen D, et al. Assessment of myocardial viability with 3D MRI at 3 T. AJR Am J Roentgenol 2009;192(6):1645–50.
30. Peters DC, Appelbaum EA, Nezafat R, et al. Left ventricular infarct size, peri-infarct zone, and papillary scar measurements: a comparison of high-resolution 3D and conventional 2D late gadolinium enhancement cardiac MR. J Magn Reson Imaging 2009;30(4):794–800.
31. Viallon M, Jacquier A, Rotaru C, et al. Head-to-head comparison of eight late gadolinium-enhanced cardiac MR (LGE CMR) sequences at 1.5 tesla: from bench to bedside. J Magn Reson Imaging 2011; 34(6):1374–87.
32. Schlosser T, Hunold P, Herborn CU, et al. Myocardial infarct: depiction with contrast-enhanced MR imaging–comparison of gadopentetate and gadobenate. Radiology 2005;236(3):1041–6.
33. Wildgruber M, Stadlbauer T, Rasper M, et al. Single-dose gadobutrol in comparison with single-dose gadobenate dimeglumine for magnetic resonance imaging of chronic myocardial infarction at 3 T. Invest Radiol 2014;49:728–34.
34. Bauner KU, Reiser MF, Huber AM. Low dose gadobenate dimeglumine for imaging of chronic myocardial infarction in comparison with standard dose gadopentetate dimeglumine. Invest Radiol 2009;44(2):95–104.
35. Tumkosit M, Puntawangkoon C, Morgan TM, et al. Left ventricular infarct size assessed with 0.1 mmol/kg of gadobenate dimeglumine correlates with that assessed with 0.2 mmol/kg of gadopentetate dimeglumine. J Comput Assist Tomogr 2009; 33(3):328–33.
36. Durmus T, Schilling R, Doeblin P, et al. Gadobutrol for magnetic resonance imaging of chronic myocardial infarction: intraindividual comparison with gadopentetate dimeglumine. Invest Radiol 2012;47(3): 183–8.
37. Wagner M, Schilling R, Doeblin P, et al. Macrocyclic contrast agents for magnetic resonance imaging of chronic myocardial infarction: intraindividual comparison of gadobutrol and gadoterate meglumine. Eur Radiol 2013;23(1):108–14.
38. Doltra A, Skorin A, Hamdan A, et al. Comparison of acquisition time and dose for late gadolinium enhancement imaging at 3.0 T in patients with chronic myocardial infarction using Gd-BOPTA. Eur Radiol 2014;24:2192–200.
39. Gheorghiade M, Bonow RO. Chronic heart failure in the United States: a manifestation of coronary artery disease. Circulation 1998;97(3):282–9.
40. Jessup M, Brozena S. Heart failure. N Engl J Med 2003;348(20):2007–18.
41. Hung J, Teng TH, Finn J, et al. Trends from 1996 to 2007 in incidence and mortality outcomes of heart failure after acute myocardial infarction: a population-based study of 20,812 patients with first acute myocardial infarction in Western Australia. J Am Heart Assoc 2013;2(5):e000172.
42. Camici PG, Prasad SK, Rimoldi OE. Stunning, hibernation, and assessment of myocardial viability. Circulation 2008;117(1):103–14.
43. Beller GA. Assessment of myocardial viability. Curr Opin Cardiol 1997;12(5):459–67.
44. Wijns W, Vatner SF, Camici PG. Hibernating myocardium. N Engl J Med 1998;339(3):173–81.
45. Velazquez EJ, Lee KL, Deja MA, et al. Coronary-artery bypass surgery in patients with left ventricular dysfunction. N Engl J Med 2011;364(17):1607–16.
46. Bonow RO, Maurer G, Lee KL, et al. Myocardial viability and survival in ischemic left ventricular dysfunction. N Engl J Med 2011;364(17):1617–25.
47. Abraham A, Nichol G, Williams KA, et al. 18F-FDG PET imaging of myocardial viability in an experienced center with access to 18F-FDG and integration with clinical management teams: the Ottawa-FIVE substudy of the PARR 2 trial. J Nucl Med 2010;51(4):567–74.
48. Wagner A, Mahrholdt H, Holly TA, et al. Contrast-enhanced MRI and routine single photon emission computed tomography (SPECT) perfusion imaging for detection of subendocardial myocardial infarcts: an imaging study. Lancet 2003;361(9355): 374–9.

49. El Aidi H, Adams A, Moons KG, et al. Cardiac magnetic resonance imaging findings and the risk of cardiovascular events in patients with recent myocardial infarction or suspected or known coronary artery disease: a systematic review of prognostic studies. J Am Coll Cardiol 2014;63(11): 1031–45.
50. Schvartzman PR, Srichai MB, Grimm RA, et al. Nonstress delayed-enhancement magnetic resonance imaging of the myocardium predicts improvement of function after revascularization for chronic ischemic heart disease with left ventricular dysfunction. Am Heart J 2003;146(3):535–41.
51. Kelle S, Roes SD, Klein C, et al. Prognostic value of myocardial infarct size and contractile reserve using magnetic resonance imaging. J Am Coll Cardiol 2009;54(19):1770–7.
52. Wu KC, Zerhouni EA, Judd RM, et al. Prognostic significance of microvascular obstruction by magnetic resonance imaging in patients with acute myocardial infarction. Circulation 1998;97(8):765–72.
53. Srichai MB, Junor C, Rodriguez LL, et al. Clinical, imaging, and pathological characteristics of left ventricular thrombus: a comparison of contrast-enhanced magnetic resonance imaging, transthoracic echocardiography, and transesophageal echocardiography with surgical or pathological validation. Am Heart J 2006;152(1):75–84.
54. Yan AT, Shayne AJ, Brown KA, et al. Characterization of the peri-infarct zone by contrast-enhanced cardiac magnetic resonance imaging is a powerful predictor of post-myocardial infarction mortality. Circulation 2006;114(1):32–9.
55. Kwong RY, Sattar H, Wu H, et al. Incidence and prognostic implication of unrecognized myocardial scar characterized by cardiac magnetic resonance in diabetic patients without clinical evidence of myocardial infarction. Circulation 2008;118(10): 1011–20.
56. Kim HW, Klem I, Shah DJ, et al. Unrecognized non-Q-wave myocardial infarction: prevalence and prognostic significance in patients with suspected coronary disease. PLoS Med 2009;6(4):e1000057.
57. Schelbert EB, Cao JJ, Sigurdsson S, et al. Prevalence and prognosis of unrecognized myocardial infarction determined by cardiac magnetic resonance in older adults. JAMA 2012;308(9):890–6.
58. Child NM, Das R. Is cardiac magnetic resonance imaging assessment of myocardial viability useful for predicting which patients with impaired ventricles might benefit from revascularization? Interact Cardiovasc Thorac Surg 2012;14(4):395–8.
59. Selvanayagam JB, Kardos A, Francis JM, et al. Value of delayed-enhancement cardiovascular magnetic resonance imaging in predicting myocardial viability after surgical revascularization. Circulation 2004;110(12):1535–41.
60. Pegg TJ, Selvanayagam JB, Jennifer J, et al. Prediction of global left ventricular functional recovery in patients with heart failure undergoing surgical revascularisation, based on late gadolinium enhancement cardiovascular magnetic resonance. J Cardiovasc Magn Reson 2010;12:56.
61. Bondarenko O, Beek AM, Twisk JW, et al. Time course of functional recovery after revascularization of hibernating myocardium: a contrast-enhanced cardiovascular magnetic resonance study. Eur Heart J 2008;29(16):2000–5.
62. Canadian Cardiovascular Society Heart Failure Management Primary Panel, Moe GW, Ezekowitz JA, et al. The 2013 Canadian Cardiovascular Society Heart Failure Management Guidelines Update: focus on rehabilitation and exercise and surgical coronary revascularization. Can J Cardiol 2014; 30(3):249–63.
63. Choi KM, Kim RJ, Gubernikoff G, et al. Transmural extent of acute myocardial infarction predicts long-term improvement in contractile function. Circulation 2001;104(10):1101–7.
64. Selvanayagam JB, Jerosch-Herold M, Porto I, et al. Resting myocardial blood flow is impaired in hibernating myocardium: a magnetic resonance study of quantitative perfusion assessment. Circulation 2005;112(21):3289–96.
65. Jahnke C, Nagel E, Gebker R, et al. Prognostic value of cardiac magnetic resonance stress tests: adenosine stress perfusion and dobutamine stress wall motion imaging. Circulation 2007;115(13):1769–76.
66. Ingkanisorn WP, Kwong RY, Bohme NS, et al. Prognosis of negative adenosine stress magnetic resonance in patients presenting to an emergency department with chest pain. J Am Coll Cardiol 2006;47(7):1427–32.
67. Klem I, Heitner JF, Shah DJ, et al. Improved detection of coronary artery disease by stress perfusion cardiovascular magnetic resonance with the use of delayed enhancement infarction imaging. J Am Coll Cardiol 2006;47(8):1630–8.
68. Bekkers SC, Yazdani SK, Virmani R, et al. Microvascular obstruction: underlying pathophysiology and clinical diagnosis. J Am Coll Cardiol 2010;55(16): 1649–60.
69. Kidambi A, Mather AN, Motwani M, et al. The effect of microvascular obstruction and intramyocardial hemorrhage on contractile recovery in reperfused myocardial infarction: insights from cardiovascular magnetic resonance. J Cardiovasc Magn Reson 2013;15(1):58.
70. Gerber BL, Rochitte CE, Melin JA, et al. Microvascular obstruction and left ventricular remodeling early after acute myocardial infarction. Circulation 2000;101(23):2734–41.
71. Nijveldt R, Beek AM, Hirsch A, et al. Functional recovery after acute myocardial infarction: comparison

between angiography, electrocardiography, and cardiovascular magnetic resonance measures of microvascular injury. J Am Coll Cardiol 2008;52(3):181–9.
72. Ito H, Maruyama A, Iwakura K, et al. Clinical implications of the 'no reflow' phenomenon. A predictor of complications and left ventricular remodeling in reperfused anterior wall myocardial infarction. Circulation 1996;93(2):223–8.
73. de Waha S, Desch S, Eitel I, et al. Relationship and prognostic value of microvascular obstruction and infarct size in ST-elevation myocardial infarction as visualized by magnetic resonance imaging. Clin Res Cardiol 2012;101(6):487–95.
74. Weinsaft JW, Kim HW, Shah DJ, et al. Detection of left ventricular thrombus by delayed-enhancement cardiovascular magnetic resonance prevalence and markers in patients with systolic dysfunction. J Am Coll Cardiol 2008;52(2):148–57.
75. Fuster V, Halperin JL. Left ventricular thrombi and cerebral embolism. N Engl J Med 1989;320(6):392–4.
76. Greaves SC, Zhi G, Lee RT, et al. Incidence and natural history of left ventricular thrombus following anterior wall acute myocardial infarction. Am J Cardiol 1997;80(4):442–8.
77. Schmidt A, Azevedo CF, Cheng A, et al. Infarct tissue heterogeneity by magnetic resonance imaging identifies enhanced cardiac arrhythmia susceptibility in patients with left ventricular dysfunction. Circulation 2007;115(15):2006–14.
78. Heidary S, Patel H, Chung J, et al. Quantitative tissue characterization of infarct core and border zone in patients with ischemic cardiomyopathy by magnetic resonance is associated with future cardiovascular events. J Am Coll Cardiol 2010;55(24):2762–8.
79. Sciagra R, Bisi G, Santoro GM, et al. Comparison of baseline-nitrate technetium-99m sestamibi with rest-redistribution thallium-201 tomography in detecting viable hibernating myocardium and predicting post-revascularization recovery. J Am Coll Cardiol 1997;30(2):384–91.
80. Bax JJ, Cornel JH, Visser FC, et al. Prediction of improvement of contractile function in patients with ischemic ventricular dysfunction after revascularization by fluorine-18 fluorodeoxyglucose single-photon emission computed tomography. J Am Coll Cardiol 1997;30(2):377–83.
81. Klein C, Nekolla SG, Bengel FM, et al. Assessment of myocardial viability with contrast-enhanced magnetic resonance imaging: comparison with positron emission tomography. Circulation 2002;105(2):162–7.
82. Heijenbrok-Kal MH, Fleischmann KE, Hunink MG. Stress echocardiography, stress single-photon-emission computed tomography and electron beam computed tomography for the assessment of coronary artery disease: a meta-analysis of diagnostic performance. Am Heart J 2007;154(3):415–23.
83. Baer FM, Theissen P, Crnac J, et al. Head to head comparison of dobutamine-transoesophageal echocardiography and dobutamine-magnetic resonance imaging for the prediction of left ventricular functional recovery in patients with chronic coronary artery disease. Eur Heart J 2000;21(12):981–91.
84. Sandstede JJ, Bertsch G, Beer M, et al. Detection of myocardial viability by low-dose dobutamine cine MR imaging. Magn Reson Imaging 1999;17(10):1437–43.
85. Cwajg JM, Cwajg E, Nagueh SF, et al. End-diastolic wall thickness as a predictor of recovery of function in myocardial hibernation: relation to rest-redistribution T1-201 tomography and dobutamine stress echocardiography. J Am Coll Cardiol 2000;35(5):1152–61.
86. Koyama Y, Matsuoka H, Mochizuki T, et al. Assessment of reperfused acute myocardial infarction with two-phase contrast-enhanced helical CT: prediction of left ventricular function and wall thickness. Radiology 2005;235(3):804–11.
87. Gerber BL, Belge B, Legros GJ, et al. Characterization of acute and chronic myocardial infarcts by multidetector computed tomography: comparison with contrast-enhanced magnetic resonance. Circulation 2006;113(6):823–33.
88. Deseive S, Bauer RW, Lehmann R, et al. Dual-energy computed tomography for the detection of late enhancement in reperfused chronic infarction: a comparison to magnetic resonance imaging and histopathology in a porcine model. Invest Radiol 2011;46(7):450–6.
89. Kartje JK, Schmidt B, Bruners P, et al. Dual energy CT with nonlinear image blending improves visualization of delayed myocardial contrast enhancement in acute myocardial infarction. Invest Radiol 2013;48(1):41–5.
90. Wichmann JL, Bauer RW, Doss M, et al. Diagnostic accuracy of late iodine-enhancement dual-energy computed tomography for the detection of chronic myocardial infarction compared with late gadolinium-enhancement 3-T magnetic resonance imaging. Invest Radiol 2013;48(12):851–6.
91. Wichmann JL, Hu X, Kerl JM, et al. Non-linear blending of dual-energy CT data improves depiction of late iodine enhancement in chronic myocardial infarction. Int J Cardiovasc Imaging 2014;30:1145–50.
92. Nensa F, Poeppel TD, Beiderwellen K, et al. Hybrid PET/MR imaging of the heart: feasibility and initial results. Radiology 2013;268(2):366–73.